

Elastic scattering by planar fractures

Thomas E. Blum*, Boise State University, Roel Snieder, Colorado School of Mines, Kasper van Wijk, Boise State University, and Mark E. Willis, ConocoPhillips

SUMMARY

Remote sensing of fractures with elastic waves is important in fields ranging from seismology to non-destructive testing. While previous analytic descriptions of scattering mostly concern very large or very small fractures (compared to the dominant wavelength), we present an analytic solution for the scattering of elastic waves from a fracture of arbitrary size. Based on the linear-slip model for a fracture, we derive the scattered amplitude in the frequency domain under the Born approximation for all combinations of incident and scattered wave modes. Our analytic results match laser-based ultrasonic laboratory measurements of a single fracture in clear plastic, allowing us to quantify the compliance of a fracture.

INTRODUCTION

Faults and fractures in the subsurface can act as conduits or barriers to fluid flow of hydrocarbons and water. Understanding the interaction of fractures with elastic waves is crucial in order to characterize fracture properties remotely. In hydrocarbon reservoirs, hydraulic fractures are generated to stimulate production and can be monitored with active or passive sources (Wills et al., 1992; Meadows and Winterstein, 1994). Besides geophysical applications, scattering from fractures is important in non-destructive testing applications (Langenberg et al., 2002).

The linear slip model links the discontinuity of the displacement field at the fracture plane to the stress traction assumed to be continuous across the slip interface (Schoenberg, 1980). This model can be directly applied to fractures of large spatial extent compared to the wavelength. The extreme case where the fracture plane is infinite leads to frequency dependent reflection and transmission coefficients (Pyrak-Nolte et al., 1990; Pyrak-Nolte and Nolte, 1992; Zhu and Snieder, 2002). The linear slip model is often used in the case of a linear slip interface (Coates and Schoenberg, 1995), or fluid-filled fractures (Groenenboom and Falk, 2000). Finally, Fang et al. (2010) present finite-difference numerical simulations of the scattering of P-waves by a finite circular fracture.

Here, we apply the linear slip model to a single finite planar fracture under the Born approximation. From this, we develop an analytic expression for the general scattered amplitude without making assumptions about the fracture size or wavelength. We derive the scattered amplitude expression in the frequency domain for incoming and scattered P-waves. We illustrate this theoretical work with a novel laboratory experiment by estimating the normal compliance for a single crack generated in a clear plastic sample, and show that the measured scattered amplitude is explained by a reasonable compliance value.

GENERAL EXPRESSIONS FOR SCATTERING BY A FRACTURE

The derivation is formulated in the frequency domain using the following Fourier convention $f(t) = \int F(\omega)e^{-i\omega t}d\omega$. For brevity, we do not make the frequency dependence explicit, and we use the Einstein summation convention.

We derive a general expression of the wave scattered by a fracture of arbitrary size. The stress across the fracture is continuous, but the displacement across the fracture is not necessarily continuous. We denote the discontinuity in the displacement by $[\mathbf{u}]$. According to equation (3.2) of Aki and Richards (2002), the displacement at location \mathbf{x} due to the discontinuity of the displacement at the fracture Σ is given by

$$u_n(\mathbf{x}) = \iint_{\Sigma} [u_i(\mathbf{s})] c_{ijkl} f_j G_{nk,l}(\mathbf{x}, \mathbf{s}) d^2s, \quad (1)$$

where $\hat{\mathbf{f}}$ is the normal vector to the fracture as shown in Figure 1, c_{ijkl} is the elasticity tensor, and $G_{nk,l}$ is the gradient of the displacement Green's function defined as

$$G_{nk,l}(\mathbf{x}, \mathbf{s}) = \frac{\partial G_{nk}(\mathbf{x}, \mathbf{s})}{\partial s_l}. \quad (2)$$

We next relate the discontinuity in the displacement to the stress field. We follow Schoenberg (1980) and assume that the slip discontinuity is related to the traction \mathbf{T} at the fracture by a compliance matrix η

$$[u_i] = \eta_{ir} T_r. \quad (3)$$

Expressing the traction with the stress σ_{ij} and the normal vector to the fracture yields

$$[u_i] = \eta_{ir} \sigma_{rs} f_s. \quad (4)$$

Inserting this result in equation (1) gives

$$u_n(\mathbf{x}) = \iint_{\Sigma} \sigma_{ij} N_{ijkl} G_{nk,l}(\mathbf{x}, \mathbf{s}) d^2s, \quad (5)$$

with

$$N_{ijkl} = \eta_{pi} f_j f_q c_{pqkl}. \quad (6)$$

We now assume that the properties of the fracture can be characterized by a normal compliance η_N and a shear compliance η_T . In that case, one can use a dyadic decomposition to write the compliance matrix as

$$\eta_{ij} = \eta_N f_i f_j + \eta_T (\delta_{ij} - f_i f_j), \quad (7)$$

where δ_{ij} is the Kronecker delta. We solve this integral equation in the Born approximation by replacing the stress in the right hand side of equation (5) by the stress $\sigma_{ij}^{(0)}$ for a P-wave propagating through a homogeneous medium, depending on

Elastic scattering by planar fractures

the type of incident wave. In that case the scattered wave is given by

$$u_n(\mathbf{x}) = \iint_{\Sigma} \sigma_{ij}^{(0)} N_{ijkl} G_{nk,l}(\mathbf{x}, \mathbf{s}) d^2s. \quad (8)$$

Since N_{ijkl} is known we can solve the scattering problem using the Born approximation.

Consider first an incoming plane P-wave that propagates in the $\hat{\mathbf{n}}$ -direction (Figure 1). Since such a wave is polarized in the longitudinal direction,

$$\mathbf{u}^{(P)}(\mathbf{s}) = \hat{\mathbf{n}} e^{ik_{\alpha}(\hat{\mathbf{n}} \cdot \mathbf{s})}, \quad (9)$$

where

$$k_{\alpha} = \omega / \alpha, \quad (10)$$

with α the P-wave velocity and ω the angular frequency. For an isotropic medium $\sigma_{ij} = \lambda \delta_{ij} \partial_k u_k + \mu (\partial_i u_j + \partial_j u_i)$ and the stress associated with this plane P-wave is

$$\sigma_{ij}^{(P)} = ik_{\alpha} (\lambda \delta_{ij} + 2\mu n_i n_j) e^{ik_{\alpha}(\hat{\mathbf{n}} \cdot \mathbf{s})}. \quad (11)$$

Inserting the stress (11) into expression (8) gives the scattered field for an incoming P-wave.

SCATTERED AMPLITUDES

The scattered field can effectively be expressed by a scattered amplitude (Merzbacher, 1970). According to expression (8), the scattered field depends on $G_{nk,l}$, which is the gradient of the Green's function. Expression (4.29) of Aki and Richards (2002) gives the gradient of the Green's function in the time domain for a homogeneous, isotropic infinite space. Retaining the P-wave far field term only, and replacing the time derivative with $-i\omega$ gives, in the frequency domain

$$G_{nk,l}(\mathbf{x}, \mathbf{s}) = \frac{-i\omega m_k m_n m_l}{4\pi\rho\alpha^3 r} e^{ik_{\alpha}r}, \quad (12)$$

where the unit vector $\hat{\mathbf{m}}$ defines the direction of the outgoing wave (Figure 1) and $r = |\mathbf{x} - \mathbf{s}|$ denotes the distance between the observation point \mathbf{x} and the integration point \mathbf{s} on the fracture,

If we momentarily choose the origin of our coordinate system to be the center of the fracture, the distance from the origin to the observation point is denoted by R . When this distance is large compared to the size of the fracture, we can approximate

$$r = R - (\hat{\mathbf{m}} \cdot \mathbf{s}), \quad (13)$$

where $\hat{\mathbf{m}}$ is the unit vector from the center of the fracture to the observation point \mathbf{x} (Figure 1). In expression (12) we replace r by equation (13) in the exponents, and replace r in the denominator by R . Inserting these results into equation (8) gives the following expressions for the radiated P-waves

$$u_n^{(P)}(\mathbf{x}) = \iint_{\Sigma} \sigma_{ij}^{(0)} N_{ijkl} e^{-ik_{\alpha}(\hat{\mathbf{m}} \cdot \mathbf{s})} d^2s \left(\frac{-i\omega m_n m_k m_l}{4\pi\rho\alpha^3} \right) \frac{e^{ik_{\alpha}R}}{R}, \quad (14)$$

In this expression $\sigma_{ij}^{(0)}$ is given by equation (11). We next define the scattered amplitude f for outgoing P-waves by

$$u_n^{(P)}(\mathbf{x}) = f_{PP} \frac{e^{ik_{\alpha}R}}{R} m_n, \quad (15)$$

In the following $f_{P,P}$ is the scattered amplitude from an incident P-wave into a scattered P-wave. A comparison with equation (14) shows that the scattered amplitude is given by

$$f_{PP} = \iint_{\Sigma} \sigma_{ij}^{(0)} N_{ijkl} e^{-ik_{\alpha}(\hat{\mathbf{m}} \cdot \mathbf{s})} d^2s \left(\frac{-i\omega m_k m_l}{4\pi\rho\alpha^3} \right), \quad (16)$$

In the following expressions it is convenient to use a form factor $F(\mathbf{k})$ that is defined as

$$F(\mathbf{k}) = \frac{\iint_{\Sigma} e^{i(\mathbf{k} \cdot \mathbf{s})} d^2s}{\iint_{\Sigma} d^2s} = A^{-1} \iint_{\Sigma} e^{i(\mathbf{k} \cdot \mathbf{s})} d^2s, \quad (17)$$

where A is the surface area of the fracture. Explicit expressions for the scattered amplitude follow by inserting expressions (7) and (11) into the equation above. This gives the following scattered amplitude for P to P scattering

$$\begin{aligned} f_{P,P}(\hat{\mathbf{n}}; \hat{\mathbf{m}}) = & \frac{\omega^2}{4\pi\rho\alpha^4} A F(k_{\alpha}(\hat{\mathbf{n}} - \hat{\mathbf{m}})) \left\{ \lambda^2 \eta_N \right. \\ & + 2\lambda\mu\eta_N \left((\hat{\mathbf{n}} \cdot \hat{\mathbf{f}})^2 + (\hat{\mathbf{m}} \cdot \hat{\mathbf{f}})^2 \right) \\ & + 4\mu^2(\eta_N - \eta_T) (\hat{\mathbf{n}} \cdot \hat{\mathbf{f}})^2 (\hat{\mathbf{m}} \cdot \hat{\mathbf{f}})^2 \\ & \left. + 4\mu^2\eta_T (\hat{\mathbf{n}} \cdot \hat{\mathbf{m}}) (\hat{\mathbf{n}} \cdot \hat{\mathbf{f}}) (\hat{\mathbf{m}} \cdot \hat{\mathbf{f}}) \right\}, \quad (18) \end{aligned}$$

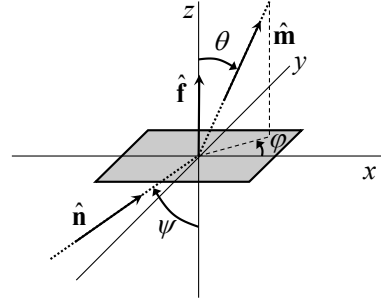


Figure 1: Definition of directions and angles for incoming and outgoing waves from a fracture (shaded area).

SCATTERING BY A PLANE CRACK

We next derive explicit expressions for the scattered amplitudes in terms of the directions of the incoming and scattered waves for the special case of a plane crack that is circular. We can show that for a circular fracture with radius a

$$F(\mathbf{k}) = \frac{2}{k_{\parallel} a} J_1(k_{\parallel} a) \quad (\text{circular fracture}), \quad (19)$$

where J_1 is the Bessel function of order 1, k_{\parallel} is the absolute value of the component of \mathbf{k} parallel to the crack, and a is the size of the crack. In order to express the scattered amplitude in the angles that define the incoming and outgoing waves we

Elastic scattering by planar fractures

need to define these angles and the orientation of the fracture. We use a coordinate system where the z -axis is perpendicular to the fracture, and the x -axis is chosen in such a way that the incoming wave propagates in the (x, z) plane coming from the $-x$ direction (Figure 1). The direction of incoming wave makes an angle ψ with the z -axis, while the direction of the outgoing wave is defined by the angles θ and φ commonly used in a spherical coordinate system. Inserting the angles defined in Figure 1 into expression (18) gives the angular dependence of the scattered amplitude

$$f_{P,P}(\hat{\mathbf{n}}; \hat{\mathbf{m}}) = \frac{\omega^2}{4\pi\rho\alpha^4} AF(k_\alpha(\hat{\mathbf{n}} - \hat{\mathbf{m}})) \times \left\{ (\lambda + \mu)^2 \eta_N \right. \\ \left. + \eta_N (\lambda\mu + \mu^2) (\cos 2\psi + \cos 2\theta) \right. \\ \left. + \mu^2 \eta_N \cos 2\psi \cos 2\theta \right. \\ \left. + \mu^2 \eta_T \sin 2\psi \sin 2\theta \cos \varphi \right\}. \quad (20)$$

In the following we consider a source normal to the fracture ($\psi = 0$), and a receiver in the $(x-z)$ plane, therefore $\phi = 0$ and $\hat{\mathbf{m}} = \sin \theta \hat{\mathbf{x}} + \cos \theta \hat{\mathbf{z}}$. Equation (20) therefore simplifies into

$$f_{P,P}(\hat{\mathbf{n}}; \hat{\mathbf{m}}) = \frac{\omega^2}{4\pi\rho\alpha^4} AF(k_\alpha(\hat{\mathbf{n}} - \hat{\mathbf{m}})) \eta_N \left[(\lambda + \mu)^2 \right. \\ \left. + \mu^2 \cos 2\theta + \mu(\lambda + \mu)(1 + \cos 2\theta) \right].$$

Note that here the term containing η_T vanishes, and the scattered amplitude $f_{P,P}(\psi = 0, \theta)$ only depends on the normal component η_N of the compliance tensor. On the other hand, for a non-normal incidence ψ , the scattered amplitude $f_{P,P}$ is a function of η_N and η_T . Moreover, for a circular fracture, we can use Equation (19)

$$F(k_\alpha(\hat{\mathbf{n}} - \hat{\mathbf{m}})) \approx \frac{-2\alpha}{a\omega \sin \theta} J_1\left(\frac{\omega a}{\alpha} \sin \theta\right). \quad (21)$$

For the experimental case, the scattered amplitude is thus expressed as

$$f_{P,P}(\theta) = \frac{-\omega a}{2\rho\alpha^3 \sin \theta} J_1\left(\frac{\omega a}{\alpha} \sin \theta\right) \eta_N \left[(\lambda + \mu)^2 \right. \\ \left. + \mu^2 \cos 2\theta + \mu(\lambda + \mu)(1 + \cos 2\theta) \right]. \quad (22)$$

LABORATORY EXPERIMENTS

We carry out laboratory experiments in order to measure P to P scattering and test our theoretical model. We use ultrasonic frequencies in plastic samples. The samples are Poly(methyl methacrylate) (PMMA) cylinders 2 in (50.8 mm) in diameter and 150 mm in height. Elastic waves are generated with a 5 MHz piezoelectric transducer (PZT), disk-shaped with a diameter of 7.5 mm. The transducer is attached to the curved surface of the cylinder using phenyl salicylate as a glue. Because this chemical has a melting point of 41.5°C, medium heating is enough to melt it and allows to attach the transducer to a curved surface. The PZT is driven by a 400 V pulse with maximum energy at the natural frequency of the PZT.

We measure the elastic displacement with a laser interferometer. Our adaptive laser ultrasonic receiver is based on a constant-wave doubled Nd:YAG laser, generating a Constant Wave (CW) 250 mW beam at a wavelength of 532 nm. The receiver uses two-wave mixing in a photorefractive crystal to deliver the displacement of the sample surface. This receiver measures the out-of-plane (vertical) displacement field. It is calibrated to output the absolute displacement field in nanometers (See Blum et al. (2010) for a complete description). The frequency response is flat between 20 kHz and 20 MHz, and it can accurately detect displacements of the order of parts of Ångströms. Since the sample material is transparent for green light, we apply a reflective tape to the surface to reflect enough light back to the laser receiver.

Measurements on a blank sample

We first carry an experiment out on a blank cylinder. This measurement is used as a reference of the background field propagating in absence of a scatterer. The sample is mounted on a computer-controlled rotational stage. We focus the laser receiver beam on the sample in a plane normal to the cylinder axis (taken as the y axis) and containing the PZT source; the $(x-z)$ plane. By computer-controlled rotation of the stage, we measure the elastic field in this plane every degree with respect to the center of the cylinder, except for a small range of angles blocked by the PZT source. For each receiver location, 256 waveforms are acquired and averaged after digitization.

The left plot of Figure 2 shows the raw ultrasonic displacement field for all recorded azimuths. The horizontal axis represents the angle δ between the source and the receiver directions, $\delta = \theta + 180^\circ$ (for θ defined in Figure 1). The main events on this scan are the direct P-wave displacement with a curved moveout and the Rayleigh wave traveling around the sample with the linear moveout. In order to remove the high amplitude Rayleigh wave arrival, we apply an f-k filter to the data. All measurements following these are performed in the $(x-z)$ plane and f-k filtered. From these data we obtain the elastic properties of the material.

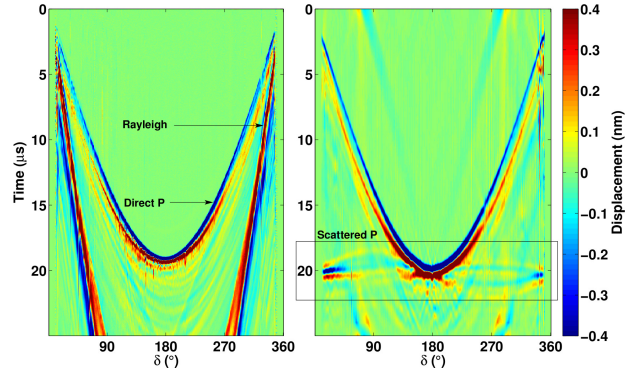


Figure 2: Displacement field for a homogeneous PMMA sample.

Fractured sample

We create a single fracture in a different cylinder of PMMA by

Elastic scattering by planar fractures

focusing a high power Q-switched Nd:YAG laser in the sample. The laser generates a short pulse (~ 20 ns) of infrared (IR) light that is absorbed by the sample material at the focal point and is converted into heat. The sudden thermal expansion generates stress and forms a fracture parallel to the cylindrical axis (Zadler and Scales (2008) give a more extensive description of the generation process). The created fracture has a circular shape and a radius of approximately 5 mm, a photograph is shown in Figure 3, with the fracture roughly in the center.

We display in on the right plot of Figure 2 the ultrasonic displacement after f-k filtering, measured with the PZT source at location S1 normal to the fracture plane, corresponding to an angle $\psi = 0^\circ$. In addition to the events present with the blank sample, we see an arrival at $\sim 20 \mu\text{s}$. This arrival corresponds to the PP scattered field from the crack. We also see that the amplitude of this event is maximum for $\delta = 180^\circ$ (forward scattering), and $\delta = 0^\circ$ (back-scattering), corresponding to the specular reflection. Finally, we note that this event is slightly asymmetric: for receiver angles $\delta < 180^\circ$, the scattering arrival is earlier than $20 \mu\text{s}$, whereas for angles $\delta > 180^\circ$, the arrival is after $20 \mu\text{s}$. This is due to the fact that the fracture is not perfectly centered on the y-axis. As we will see in the next section, for this source position the scattered amplitude is a function of η_N only.

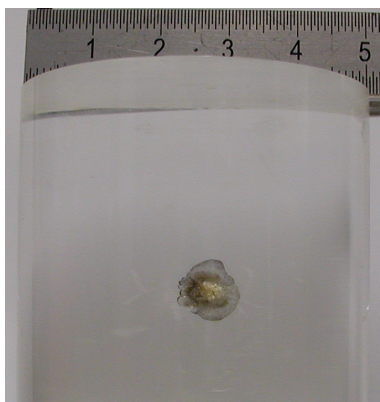


Figure 3: Photograph of the disk-shaped fracture in our laboratory sample. Ruler units are cm. The diameter of the fracture is approximately 10 mm, and the diameter of the cylinder is 50.8 mm.

Scattered amplitudes

The theoretical scattered amplitude for the experimental setup is given by 22. To compare the experimental results with the analytic expression, we first apply a narrow band-pass filter centered around $f_0 = 1$ MHz, corresponding to the dominant frequency of the scattered event. We then pick the amplitude of the scattered arrival at its maximum for a range of angles excluding traces close to the source, and receivers facing the source, where the incident and scattered field overlap. The experimental amplitude for the valid range of angles is plotted in blue in Figure 4.

We compute the corresponding theoretical amplitude for $f_0 =$

1 MHz, for a circular fracture with radius $a = 5$ mm, and using the Lamé coefficients computed from the blank measurement. We optimize the fit with the theoretical amplitude (displayed in red in the figures) for the normal incidence data since it only depends on normal component of the compliance η_N . We find that the best fit is obtained for $\eta_N \approx 10^{-11}$ m/Pa, corresponding to the thick dashed red curve in Figure 4. We also plot the theoretical curves for $\eta_N = 2 \cdot 10^{-11}$ m/Pa and $\eta_N = 0.5 \cdot 10^{-11}$ m/Pa in dotted purple and orange, respectively, to show that the $\eta_N = 10^{-11}$ m/Pa value is a robust fit. This value of compliance is in the same range as $\eta \sim 10^{-12} - 10^{-9}$ m/Pa found in the literature in the case of a single fracture in steel (Pyrak-Nolte and Nolte, 1992) and a fault zone (Zhu and Snieder, 2002).

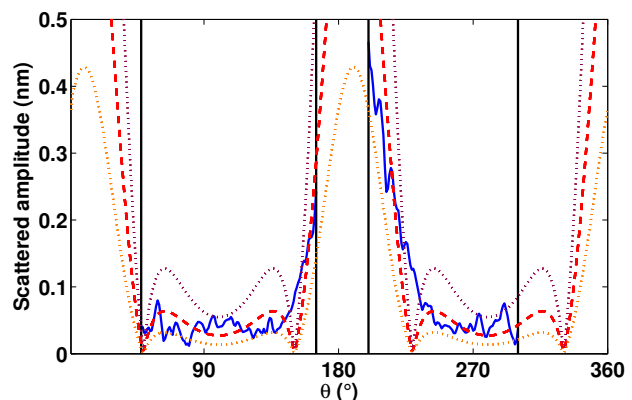


Figure 4: Scattered amplitude for the source at normal incidence in blue ($\psi = 0^\circ$). The best theoretical fit corresponding to $\eta_N = 10^{-11}$ m/Pa is plotted in thick dashed red. We also show the theoretical amplitudes corresponding to half (dotted orange) and twice (dotted purple) this value of η_N .

CONCLUSIONS

Based on a linear-slip model, we derive the analytic expression of the scattered amplitude of a plane fracture of arbitrary size under the Born approximation. Of particular interest are the results for fractures of comparable size to the elastic wavelength.

The theory provides scattered amplitudes expressed as a product of a Bessel function and trigonometric functions in the case of a circular fracture. Non-contacting ultrasonic data acquired on a plastic laboratory sample for P-P scattering from a circular fracture is in qualitative agreement with the theory, and the estimated compliance of the fracture agrees with values reported in the literature.

ACKNOWLEDGMENTS

We thank ConocoPhillips, especially Phil Anno, for supporting this research; as well as John Scales from Colorado School of Mines and fellow members of the Physical Acoustics Laboratory for their constructive ideas and comments.